MPMI Vol. 24, No. 2, 2011, pp. 183–193. doi:10.1094/MPMI-07-10-0149. *e*-Xtra*

Callose Deposition: A Multifaceted Plant Defense Response

Estrella Luna,[1] Victoria Pastor,[3] Jérôme Robert,[2] Victor Flors,[3] Brigitte Mauch-Mani,[2] and Jurriaan Ton[1]

[1]Department of Biological Chemistry, Rothamsted Research, Harpenden AL5 2JQ U.K.; [2]Institute of Botany, University of Neuchâtel, Neuchâtel, CH-2009 Switzerland; [3]Plant Physiology Section, CAMN Department, University of Jaume I, Castellón, 12071 Spain

Submitted 2 July 2010. Accepted 8 October 2010.

Callose deposition in *Arabidopsis* has emerged as a popular model system to quantify activity of plant immunity. However, there has been a noticeable rise in contradicting reports about the regulation of pathogen-induced callose. To address this controversy, we have examined the robustness of callose deposition under different growth conditions and in response to two different pathogen-associated molecular patterns, the flagellin epitope Flg22 and the polysaccharide chitosan. Based on a commonly used hydroponic culture system, we found that variations in growth conditions have a major impact on the plant's overall capacity to deposit callose. This environmental variability correlated with levels of hydrogen peroxide (H_2O_2) production. Depending on the growth conditions, pretreatment with abscissic acid stimulated or repressed callose deposition. Despite a similar effect of growth conditions on Flg22- and chitosan-induced callose, both responses showed differences in timing, tissue responsiveness, and colocalization with H_2O_2. Furthermore, mutant analysis revealed that Flg22- and chitosan-induced callose differ in the requirement for the NADPH oxidase RBOHD, the glucosinolate regulatory enzymes VTC1 and PEN2, and the callose synthase PMR4. Our study demonstrates that callose is a multifaceted defense response that is controlled by distinct signaling pathways, depending on the environmental conditions and the challenging pathogen-associated molecular pattern.

Plants protect themselves against pathogens by using a variety of chemical and physical defense mechanisms. Callose-containing cell-wall appositions, called papillae, are effective barriers that are induced at the sites of attack during the relatively early stages of pathogen invasion. Callose is an amorphous, high–molecular weight β-(1,3)-glucan polymer that serves as a matrix in which antimicrobial compounds can be deposited, thereby providing focused delivery of chemical defenses at the cellular sites of attack. Callose deposition is typically triggered by conserved pathogen-associated molecular patterns (PAMPs) (Brown et al. 1998; Gomez-Gomez et al. 1999a). Examples of bacterial PAMPs are the 22–amino acid sequence of the conserved N-terminal part of flagellin (Gomez-Gomez and Boller 2000) and the bacterial elongation factor EF-Tu (Elf18) (Kunze et al. 2004). Chitin, a β-(1,4)-linked polymer of *N*-acetylglucosamine, and chitosan, a randomly distributed β-(1,4)-linked polymer of D-glucosamide and acetylglucosamine, are examples of potent callose-inducing PAMPs from fungal cell walls (Iritri and Faoro 2009). Apart from PAMPs, endogenous elicitors from pathogen- or herbivore-damaged plant tissues can activate callose depositions as well. Well-known examples of damage-associated patterns (DAMP) are oligogalacturonides (OG) (Ridley et al. 2001).

The signaling pathways controlling PAMP-triggered immunity (PTI) are under the control of pathogen recognition receptors (PRR). Activity of the downstream pathways is marked by common signaling events, such as anion fluxes, protein phosphorylation cascades, accumulation of reactive oxygen species (ROS), and defense gene induction (Boller and Felix 2009; Jeworutzki et al. 2010; Nicaise et al. 2009). Recently, PAMP- or DAMP-induced callose deposition in cotyledons or leaves of *Arabidopsis* has emerged as a popular marker response to study the signaling pathways controlling PTI or the suppression of these pathways by virulence-promoting pathogen effectors (Table 1). The advantage of this model system is that it allows for rapid and relatively simple screening of PTI activity. The model system has been used to demonstrate that reactive oxygen species (ROS) act as positive signals in Flg22- and OG-induced callose (Galletti et al. 2008; Zhang et al. 2007), and recently, it was found that the RNA interference regulatory protein Argonaute1 generates various miRNA signals that stimulate or repress Flg22-induced callose (Li et al. 2010). Furthermore, Flg22-induced callose in *Arabidopsis* has been demonstrated to require intact biosynthesis of 4-methoxylated indole glucosinolates (Clay et al. 2009), suggesting that these secondary metabolites or break-down products thereof play a crucial role in the regulation of callose.

The timing and intensity of pathogen-induced callose can be influenced by environmental signals. For example, plants that are locally subjected to pathogen attack express systemic acquired resistance, which is associated with augmented levels of callose upon secondary pathogen inoculation (Kohler et al. 2002). Furthermore, resistance-inducing chemicals can augment depositions of pathogen-inducible callose. Well-known examples of such priming agents are the salicylic acid (SA) analog benzo(1,2,3) thiadiazole-7-carbothioic acid *S*-methyl ester (Kohler et al. 2002), and the nonprotein amino acid β-amino butyric acid (BABA) (Ton and Mauch-Mani 2004; Zimmerli et al. 2000). We have previously demonstrated that BABA-induced priming of callose requires an intact abscissic acid (ABA)-dependent pathway in *Arabidopsis*. Since ABA regulates plant

Estrella Luna and Victoria Pastor contributed equally to the work

Corresponding authors: Victor Flors; Telephone: +34-964729417; E-mail: flors@uji.es; Brigitte Mauch-Mani; Telephone: +41-327182205; E-mail: brigitte.mauch@unine.ch; Jurriaan Ton; Telepone: +44-1582763133; E-mail: jurriaan.ton@bbsrc.ac.uk

*The *e*-Xtra logo stands for "electronic extra" and indicates that three supplementary figures and a supplementary table are published online.

adaptation to abiotic stress, these findings suggest that pathogen-induced callose is coregulated by abiotic stress signals (Flors et al. 2005; Mauch-Mani and Mauch 2005). Indeed, in recent years, ABA has emerged as a multifaceted modulator of disease resistance (Asselbergh et al. 2008; Ton et al. 2009).

The role of ABA in disease resistance depends on a multitude of factors, such as the attacking pathogen, its specific way of gaining entry into the host, the timing of the defense response, and the type of plant tissue that is under attack. In general, ABA exerts a positive influence on early-acting defenses, such as stomatal closure, but a negative influence on later-acting defense mechanisms that are under the control of plant hormones SA and jasmonic acid (Ton et al. 2009). Nevertheless, this trend does not explain the controversial function of ABA in pathogen-induced callose. It was recently reported that ABA suppresses callose deposition in *Arabidopsis* cotyledons after treatment with the bacterial PAMP flagellin (Clay et al. 2009), which is supported by earlier findings that callose induced by *Pseudomonas syringae* pv. *tomato* is suppressed by ABA (de Torres-Zabala et al. 2007). Contrary to these findings, other groups have demonstrated a positive influence of ABA on callose deposition in response to infection by different fungal and oomycete pathogens (Asselbergh et al. 2008; Flors et al. 2005; Ton et al. 2009). In fact, a DNA/RNA nuclease was recently reported to act as a critical regulator of ABA-dependent stimulation of callose deposition during *Botrytis cinerea* infection (You et al. 2010).

In this study, we have evaluated the robustness of a widely used hydroponic *Arabidopsis* system to quantify PAMP-induced callose. Our results demonstrate that variations in abiotic growth conditions have a major impact on the plant's capacity to deposit callose in this system, which correlate with levels of H_2O_2 in the tissue. Moreover, the impact of ABA on callose deposition varied from repressive to stimulatory, depending on the growth conditions. We furthermore demonstrate that the pathways controlling callose differ according to the challenging PAMP, illustrating that pathogen-induced callose is a multifaceted defense response that is regulated by multiple signals rather than one, conserved signaling pathway.

RESULTS

Flg22- and chitosan-induced callose in hydroponically grown *Arabidopsis*.

To make a direct comparison between Flg22- and chitosan-induced callose, *Arabidopsis* seedlings were grown at an irradiance of 150 μE m^{-2} s^{-1} in hydroponic Murashige and Skoog medium containing 1% sucrose without Gamborg vitamins. At 24 h after application of 1 μM Flg22 or 0.01% chitosan (wt/vol), cotyledons were collected, stained with aniline blue, and examined by UV epifluoresence microscopy. As is illustrated in Figure 1A, both PAMP treatments caused a noticeable increase in the number of callose depositions compared with the mock treatment. However, the size of individual callose depositions in chitosan-treated plants appeared larger than those from Flg22-treated plants. To enumerate these differences, callose was quantified from digital photographs and was

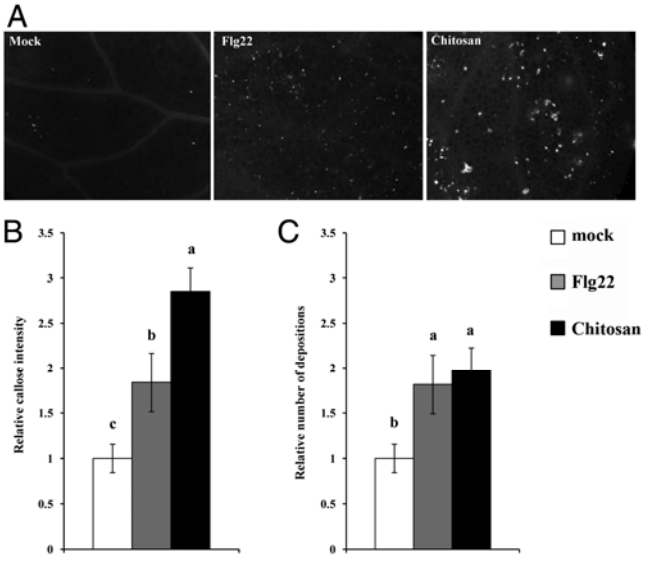

Fig. 1. Phenotype of Flg22- and chitosan-induced callose. **A,** Morphologic differences between callose depositions in cotyledons of 9-day-old *Arabidopsis* seedlings (Col-0) at 24 h after mock treatment, 1 μM Flg22 or 0.01% chitosan. Photographs of aniline blue–stained cotyledons under UV epifluorescence show representative differences in callose depositions between treatments. Seedlings were cultivated at 150 μE m^{-2} s^{-1} of light in liquid Murashige Skoog medium containing 1% sucrose without Gamborg vitamins. **B,** Relative callose intensities were quantified as the number of fluorescent callose-corresponding pixels relative to the total number of pixels covering plant material. Values represent means (± standard error of the mean (SEM); $n > 20$), standardized to the mean callose intensity in mock-treated seedlings. **C,** Relative numbers of callose depositions were quantified as the number of individual depositions per unit of cotyledon surface. Values represent means (±SEM; $n > 20$), standardized to the mean number in mock-treated seedlings. Different letters indicate statistically significant differences between treatments (Fisher's least significant differences test; $\alpha = 0.05$).

Table 1. Recent publications that have used PAMP-induced callose deposition in *Arabidopsis* as a marker for PTI activity[a]

Experimental system	PAMP	Signaling process	Reference
Application to hydroponically grown seedlings	Flg22, chitin, peptidoglycan	Induction of PTI and effector-triggered suppression of PTI in roots.	Millet et al. 2010
Infiltration in leaves	Flg22	Regulation of defense gene expression by miRNAs	Li et al. 2010
Application to hydroponically grown seedlings	Flg22, Elf18	Poly(ADP-ribosyl)ation	Adams-Phillips et al. 2010
Application to hydroponically grown seedlings	Flg22, Elf18	PRR quality control in the ER	Lu et al. 2009
Application to hydroponically grown seedlings	Flg22, Elf18	PRR quality control in the ER	Saijo et al. 2009
Infiltration in leaves	Flg22	PAMP activity by bacterial DNA	Yakushiji et al. 2009
Infiltration in leaves	Flg22	Induction of salicylic acid accumulation	Wang et al. 2009
Application to hydroponically grown seedlings	Flg22	Induction of glucosinolate metabolites	Clay et al. 2009
Infiltration in leaves	Oligogalacturonides	Reactive oxygen species signaling	Galletti et al. 2008
Infiltration in leaves	Flg22	Protein phosphorylation and reactive oxygen species signaling	Zhang et al. 2007
Infiltration in leaves	Flg22	Effector-triggered suppression of PTI via ADP ribosylation.	Fu et al. 2007
Application to hydroponically grown seedlings	Flg22	Activity of the FLS2 receptor	Dunning et al. 2007

[a] PAMP = pathogen-associated molecular pattern; PTI = PAMP-triggered immunity; PRR = pathogen recognition receptors; ER = endoplasmic reticulum.

expressed as the relative number of callose-corresponding pixels (callose intensity) or the relative number of callose depositions. Whereas the number of depositions did not differ between Flg22- and chitosan-treated seedlings, callose intensity was significantly higher in chitosan-treated seedlings than in Flg22-treated seedlings (Fig. 1B). Hence, 0.01% chitosan triggers higher amounts of callose per deposition than 1 μM Flg22. Further dose-response analysis revealed that this difference in callose morphology was also apparent at other concentrations of the applied PAMPs (Supplementary Fig. S1; data not shown). Since 1 μM flg22 and 0.01% chitosan yielded the most consistent levels of callose elicitation between independent experiments, subsequent experiments were carried out with these doses, unless stated otherwise.

Impact of growth conditions on callose deposition.

Levels of Flg22- and chitosan-induced callose in hydroponically grown *Arabidopsis* were measured under different environmental growth conditions. To minimize possible bias from unaccounted environmental conditions, results are presented from experiments with consistent outcomes in three different laboratories (Supplementary Table S1). Data presented in the figures show average values from pooled datasets. Increasing concentrations of sucrose in the growth medium had a general suppressive effect on callose deposition (Fig. 2A). Although 1 and 2.5% sucrose did not have a profound impact on the level of basal callose deposition in mock-treated seedlings, addition of 5% sucrose to the growth medium suppressed basal callose deposition by sixfold compared with plants at 0% sucrose. Moreover, Flg22-induced callose was significantly repressed at 2.5 and 5% sucrose, whereas chitosan-induced callose was already repressed at 1% sucrose in comparison to 0% sucrose. Hence, sucrose represses basal and PAMP-induced callose. Next, we investigated the effects of light on callose deposition. Seedlings grown at the relatively low light intensity of 75 μE m^{-2} s^{-1} deposited significantly lower levels of basal and Flg22-induced callose than seedlings grown at 150 μE m^{-2} s^{-1} (Fig. 2B), suggesting that light boosts basal and Flg22-induced callose. Differences in light intensity did not statistically affect quantities of chitosan-induced callose (Fig. 2B). Finally, we examined the impact of vitamins in the growth medium. Gamborg vitamins are commonly used to supplement hydroponic plant culture media. Notably, this supplement consists of a mixture of potent antioxidant vitamins, such as myo-inositol,

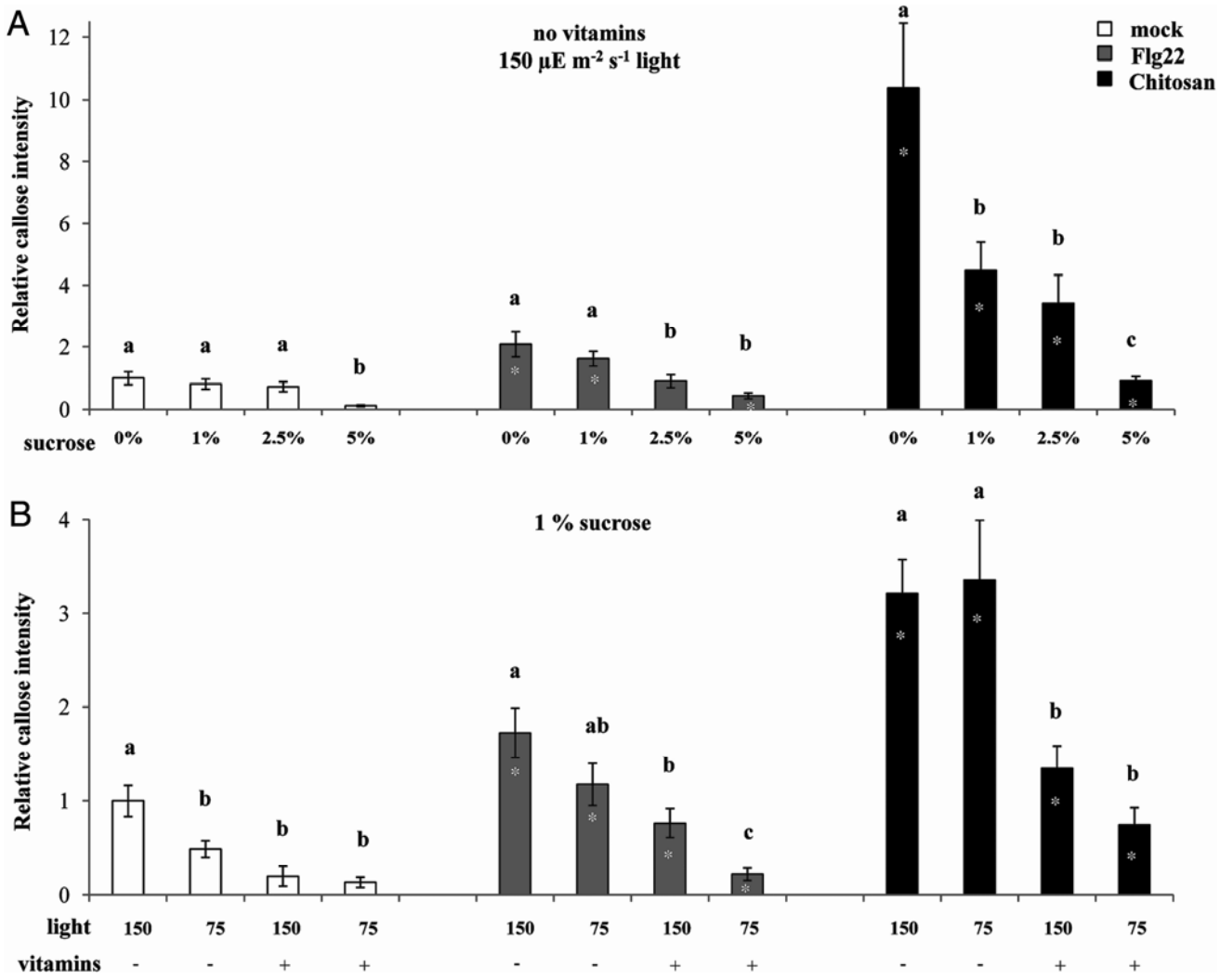

Fig. 2. Impact of growth conditions on callose deposition in cotyledons of 9-day-old *Arabidopsis* seedlings (Col-0). Data shown are average values of relative callose intensities (± standard error of the mean; $n > 20$) at 24 h after treatment with 1 μM Flg22 or 0.01 % chitosan. Values were standardized to the callose intensity in mock-treated seedlings at 150 μE m^{-2} s^{-1} of light, 1% sucrose, and without Gamborg vitamins. Different letters indicate statistically significant differences between growth conditions (Fisher's least significant differences test; $\alpha = 0.05$). Asterisks indicate statistically significant differences between pathogen-associated molecular pattern treatments and corresponding controls at similar growth conditions (Student's *t*-test; $\alpha = 0.05$). **A,** Impact of sucrose on callose deposition. **B,** Impact of light and Gamborg vitamins on callose deposition.

thiamine, and nicotinic acid (Gamborg et al. 1968). Cultivation of seedlings in medium with Gamborg vitamins drastically suppressed basal, Flg22-, and chitosan-induced callose (Fig. 2B), suggesting a positive role of ROS in callose regulation. The relative numbers of callose depositions displayed a similar responsiveness to the variable growth conditions as the relative callose intensities (data not shown). Overall, these results demonstrate that environmental growth conditions in hydroponically grown *Arabidopsis* have a profound impact on the regulation of callose deposition.

Impact of growth conditions on H_2O_2 accumulation.

Because antioxidant Gamborg vitamins suppressed basal and PAMP-induced callose (Fig. 2B), we examined to what extent this variation is related to endogenous H_2O_2 levels. To this end, seedlings were grown under different growth conditions and were fixed in acidic 3,3-diaminobenzidine (DAB) staining solution (pH < 3) at 24 h after PAMP treatment. H_2O_2 levels were quantified digitally by the relative number of dark-brown pixels after 24 h of staining. Callose-suppressive growth conditions, such as low light (75 μE m^{-2} s^{-1}), 5% sucrose, or the presence of Gamborg vitamins, suppressed basal and PAMP-induced H_2O_2 (Fig. 3). Conversely, callose-promoting growth conditions, such as high light intensity (150 μE m^{-2} s^{-1}), 1% sucrose, or lack of vitamins (Fig. 2), allowed significantly higher levels of basal and PAMP-induced H_2O_2 (Fig. 3). Hence, the observed variation in callose deposition under different growth conditions correlates with levels of H_2O_2 accumulation in the tissue.

The impact of ABA on callose deposition varies according to the growth conditions.

The role of ABA as a regulatory hormone in disease resistance has been studied extensively (Asselbergh et al. 2008; Mauch-Mani and Mauch 2005; Ton et al. 2009). Nevertheless, the role of this plant hormone in regulation of pathogen-induced callose remains controversial. To examine how closely this controversy is related to influences by abiotic growth conditions, we examined the effects of ABA application on callose under different conditions. At low light intensity (75 μE m^{-2} s^{-1}),

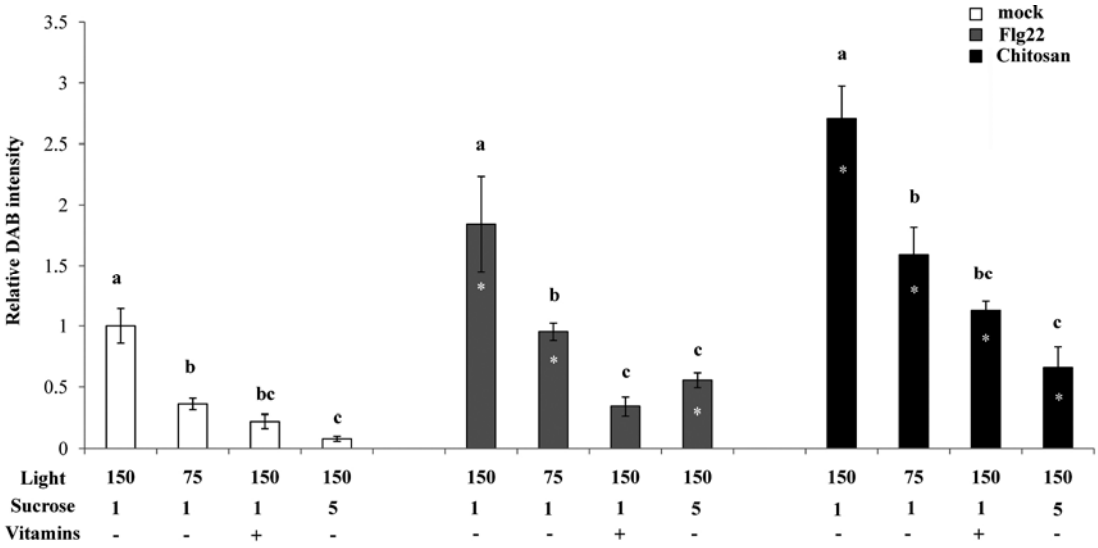

Fig. 3. Impact of growth conditions on H_2O_2 accumulation in cotyledons of 9-day-old *Arabidopsis* seedlings. Shown are average values of relative 3,3-diaminobenzidine (DAB) staining intensities (± standard error of the mean; $n > 15$) at 24 h after treatment with 1 μM Flg22 or 0.01 % chitosan. Values were standardized to the DAB intensity in mock-treated seedlings at 150 μE m^{-2} s^{-1} of light, 1% sucrose, and without Gamborg vitamins. Different letters indicate statistically significant differences between growth conditions (Fisher's least significant differences test; $\alpha = 0.05$). Asterisks indicate statistically significant differences between pathogen-associated molecular pattern treatments and corresponding controls at similar growth conditions (Student's *t*-test; $\alpha = 0.05$).

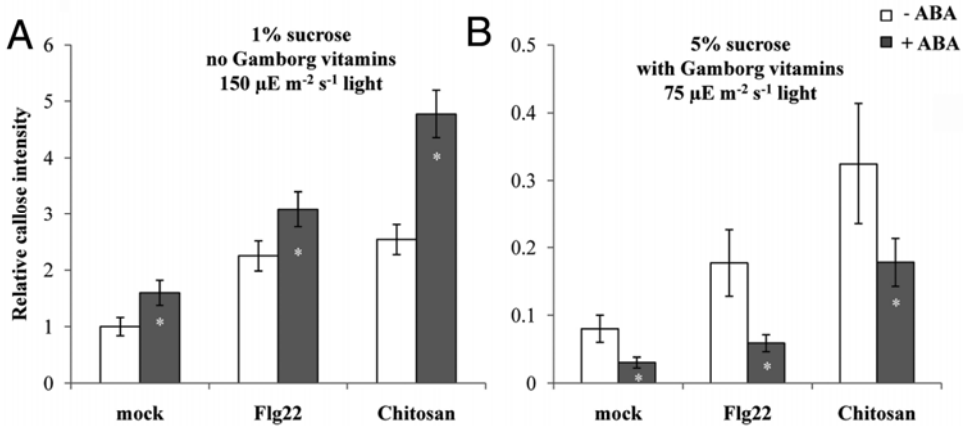

Fig. 4. Opposite impacts of abscissic acid (ABA) on callose deposition at two different growth conditions. Seedlings were treated with 5 μM ABA at 24 h prior to pathogen-associated molecular pattern (PAMP) treatment. Data shown are average values of relative callose intensities (± standard error of the mean; $n > 20$) at 24 h after PAMP treatment. Values were standardized to the callose intensity in mock-treated seedlings at 150 μE m^{-2} s^{-1} of light, 1% sucrose, without Gamborg vitamins and ABA. Asterisks indicate statistically significant changes in response to ABA treatment (Student's *t*-test; $\alpha = 0.05$).

5% sucrose, and with Gamborg vitamins, pretreatment with 5 μM ABA 24 h prior to PAMP application resulted in a repression of basal and PAMP-induced callose deposition (Fig. 4). Strikingly, when seedlings had been cultivated at high light intensity (150 μE m^{-2} s^{-1}), 1% sucrose, and without vitamins, pretreatment with ABA stimulated basal and PAMP-induced callose (Fig. 4). Similarly contrasting effects were observed upon treatment with 50 μM ABA (Table 2). To identify the exact growth conditions under which ABA represses or stimulates callose, we performed experiments under various combinations of light, sucrose, and vitamins. Only the combination of low light intensity (75 μE m^{-2} s^{-1}), 5% sucrose, and Gamborg vitamins provided conditions under which ABA suppressed callose, whereas all other conditions supported mostly stimulatory effects by ABA (Table 2). In all experiments, numbers of callose depositions responded similarly to ABA as the callose intensities (data not shown). Since the combination of low light, high sucrose, and vitamins suppresses H_2O_2 accumulation (Fig. 3), we propose that the impact of ABA on callose changes from repressive to stimulatory, depending on a threshold of cellular ROS.

Timing and localization of Flg22- and chitosan-induced H_2O_2 and callose.

To further investigate the role of ROS in PAMP-induced callose, we examined the dynamics of H_2O_2 accumulation in response to Flg22 and chitosan in a time-series experiment. Seedlings were cultivated at callose- and H_2O_2-promoting growth conditions (1% sucrose, 150 μE m^{-2} s^{-1} of light, no vitamins) and were fixed in acidic DAB staining solution at different timepoints after PAMP induction. Both Flg22 and chitosan strongly elicited H_2O_2 production at 30 min after application (Fig. 5A). However, Flg22-induced H_2O_2 was more transient than chitosan-induced H_2O_2, which was more sustained and lasted up to 24 h after induction treatment. In a separate experiment, we assessed the dynamics of callose deposition under similar growth conditions. Also here, the dynamics of the callose response differed considerably between both PAMP treatments. Whereas chitosan-induced callose was already apparent at 2 h after treatment, Flg22-induced callose was not significantly induced until 8 h after treatment (Fig. 5B). Hence, Flg22- and chitosan-induced callose are preceded by H_2O_2 accumulation, but the dynamics of both PAMP responses differs between Flg22- and chitosan-treated seedlings.

To examine tissue localization of PAMP-induced H_2O_2 and callose, seedlings were double-stained with DAB and aniline blue and were examined by a combination of light and epifluorescence microscopy (UV). As is shown in Figure 5, chitosan-induced H_2O_2 accumulated at similar sites as chitosan-induced callose. On the other hand, no obvious colocalization between H_2O_2 and callose was observed after treatment with Flg22. This lack of colocalization may be caused by the more transient nature of Flg22-induced H_2O_2 accumulation (Fig. 6).

Next, we investigated the sensitivity by which different plant tissues deposit PAMP-induced callose in the hydroponic growth medium. Millet and associates (2010) recently reported that Flg22, chitin, and peptidoglycan trigger different patterns of callose deposition in roots of hydroponically growth *Arabidopsis* seedlings. Surprisingly, however, we did not find a significant increase in root callose upon treatment with Flg22, while chitosan triggered a strong and statistically significant root callose response (Fig. 7). This differential responsiveness was consistent at different concentrations of applied PAMPs (Fig. 7). Since the Flg22 receptor FLS2 has been shown to be

Table 2. Impact of pretreatment with 50 μM abscissic acid (ABA) on basal and pathogen-associated molecular pattern (PAMP)-induced callose at different growth conditions

			Effect of ABA pretreatment[b]		
Light intensity[a]	**Sucrose (%)**	**Gamborg vitamins**	**Mock**	**Flg22**	**Chitosan**
High light	1	No	+	+	+
Low light	1	No	+	+	n.s.
High Light	5	No	n.s.	+	+
Low light	1	Yes	+	+	+
High light	1	Yes	n.s.	+	+
Low light	5	Yes	–	–	–

[a] High light = 150 μE m^{-2} s^{-1}; Low light = 75 μE m^{-2} s^{-1}.
[b] Material for callose quantifications was collected at 24 h after mock or PAMP treatment (1 μM Flg22 or 0.01 % chitosan). ABA was applied 24 h prior to mock or PAMP treatment. + = potentiation of callose by ABA; – = suppression of callose by ABA; n.s. = no statistically significant effect by ABA.

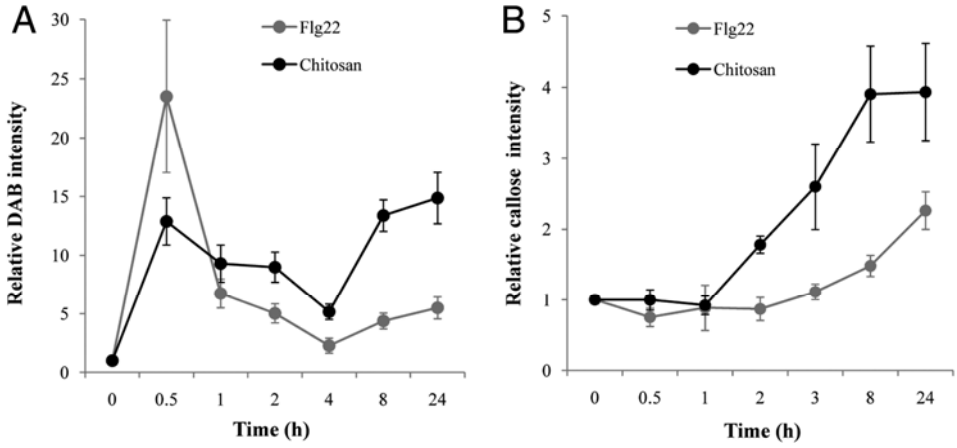

Fig. 5. Dynamics of **A,** H_2O_2 and **B,** callose deposition at different timepoints after treatment with 1 μM Flg22 or 0.01% chitosan. Shown are average values (± standard error of the mean; $n > 15$) of relative staining intensities standardized to mock treatments. Seedlings were grown under standard growth conditions at 150 μE m^{-2} s^{-1} of light, 1% sucrose, and without Gamborg vitamins.

expressed in *Arabidopsis* roots (Robatzek et al. 2006), the differential callose response to Flg22 and chitosan can only be explained by dissimilarities in the downstream signaling pathways under our growth conditions. Together with differences in colocalization between Flg22- and chitosan-induced H_2O_2 and callose (Fig. 6), these results suggest that Flg22- and chitosan-induced callose are controlled by distinct pathways.

Differential regulation of Flg22- and chitosan-induced callose.

To further investigate the pathways controlling Flg22- and chitosan-induced callose, we evaluated levels of PAMP-induced H_2O_2 and callose in mutants that are affected in ROS-scavenging and ROS-producing enzymes. The cat2-1 mutant, which is impaired in a peroxisomal catalase (Bueso et al. 2007), allowed significantly enhanced levels of PAMP-induced H_2O_2 (Fig. 8A), which correlated with enhanced levels of callose deposition (Fig. 8B). This phenotype is consistent with a potentiating function of H_2O_2 in callose deposition, since the *cat2-1* mutant is reduced in its ability to scavenge H_2O_2 (Bueso et al. 2007). In support of this, the *rbohD* mutant, carrying a T-DNA knock-out mutation in the superoxide-generating NADPH oxidase gene RBOHD (Pogany et al. 2009), accumulated reduced levels of Flg22-induced H_2O_2 and failed to deposit enhanced levels of callose upon treatment with Flg22 (Fig. 8). Surprisingly, however, *rbohD* deposited wild-type levels of callose in response to chitosan (Fig. 8B), despite an obvious reduction in chitosan-induced H_2O_2 (Fig. 8A). Similar results were obtained in response to a fivefold lower dose of chitosan (0.002%; Supplementary Fig. S2), suggesting that the intact callose response of *rbohD* to chitosan is not due to overstimulation of the defense response or phytotoxicity of chitosan. Hence, chitosan-induced callose, unlike Flg22-induced callose, functions independently of RBOHD-dependent H_2O_2. The *vtc1-1* mutant, which accumulates 10-fold lower levels of antioxidant ascorbic acid than wild-type plants (Conklin et al. 2000), also showed differential responsiveness to Flg22 and chitosan (Fig. 8B). As expected, *vtc1-1* plants allowed dramatically enhanced levels of H_2O_2 accumulation under all conditions tested (Fig. 8A), which correlated with augmented levels of basal and chitosan-induced callose in comparison with wild-type plants (Fig. 8B). However, *vtc1-1* failed to deposit increased levels of callose after treatment with Flg22 (Fig. 8B). Since ascorbic acid functions as a cofactor in myrosinase-dependent break-down of glucosinolates (Burmeister et al. 2000), the inability of *vtc1-1* to deposit enhanced callose upon Flg22 treatment confirms the earlier finding that glucosinolate metabolites regulate Flg22-induced callose (Clay et al. 2009). Accordingly, basal and chitosan-induced callose is not controlled by glucosinolate-derived metabolites.

To clarify the role of glucosinolate metabolites in callose deposition, we tested the myrosinase mutant *pen2-2*, which is blocked in production of specific glucosinolate break-down products (Bednarek et al. 2009; Clay et al. 2009). Like the *vtc1-1* mutant, *pen2-2* failed to deposit enhanced callose in response to Flg22, whereas treatment of *pen2-2* with 0.002 or 0.01% chitosan induced statistically significant enhancements in callose deposition (Fig. 8B). Hence, glucosinolate metabolites play a role in Flg22-induced callose but play no role in chitosan-induced callose deposition.

To examine the contribution of the callose synthase PMR4, we quantified levels of Flg22- and chitosan-induced callose in the *pmr4-1* mutant (Nishimura et al. 2003). As expected, *pmr4-1* deposited dramatically reduced levels of basal callose

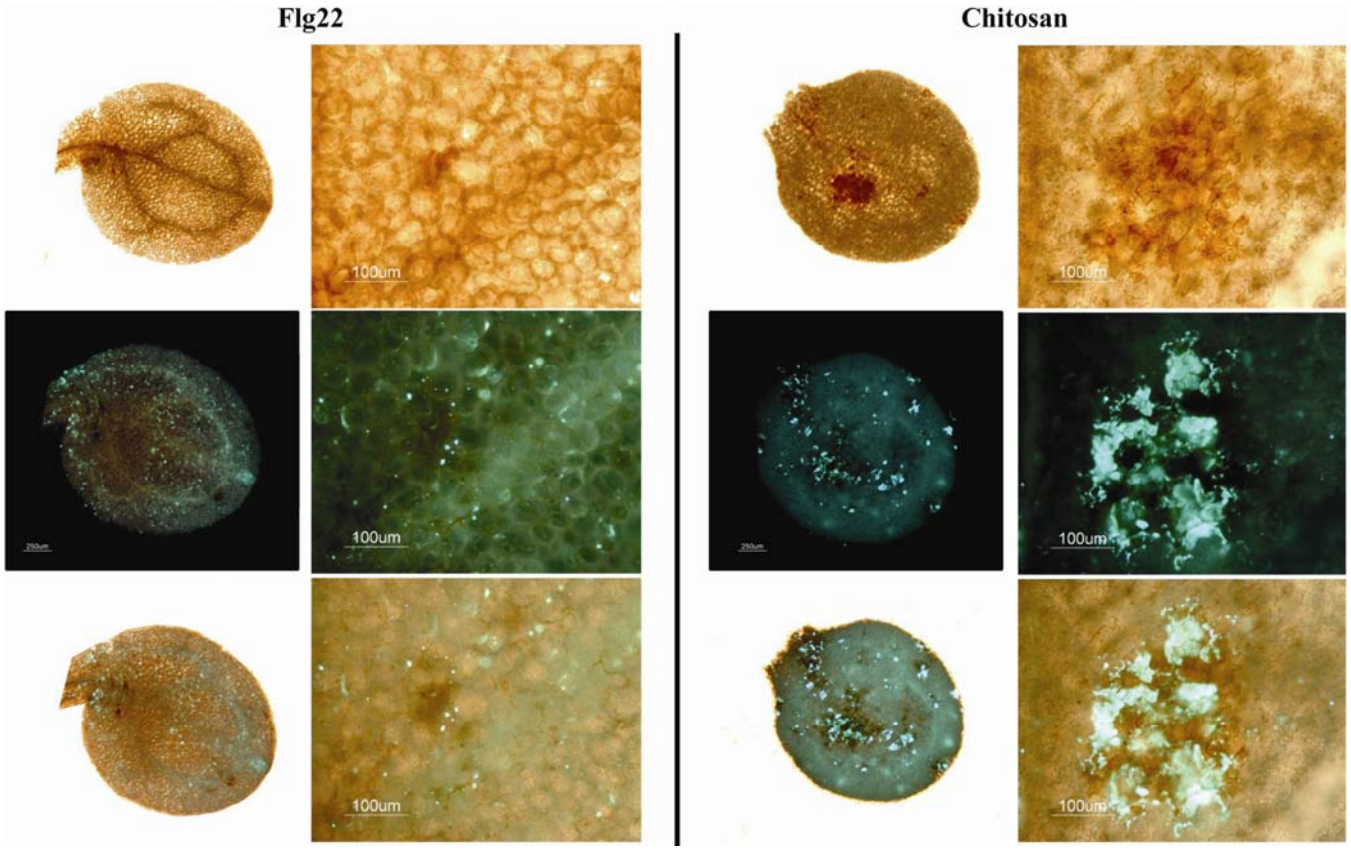

Fig. 6. Localization of H_2O_2 and callose at 24 h after treatment with 1 μM Flg22 or 0.01% chitosan. Photographs show double-stained cotyledons (3,3-diaminobenzidine and aniline-blue) exposed to a combination of bright light and UV. Seedlings were grown under150 μE m^{-2} s^{-1} light, 1% sucrose, without Gamborg vitamins.

and failed to respond to Flg22 (Fig. 9). However, chitosan elicited a residual callose response in *pmr4-1* plants, even though the absolute levels of chitosan-induced callose were reduced by 90% in comparison to the wild-type (Fig. 9). Thus, Flg22-induced callose is entirely derived from PMR4, while approximately 10% of chitosan-induced callose comes from one or more other callose synthases than PMR4.

DISCUSSION

The primary objective of this study was to evaluate the robustness and reproducibility of a widely used model system in PTI plant research, i.e., PAMP-induced callose in cotyledons of hydroponically grown *Arabidopsis* seedlings. Although exogenous application of Flg22 or chitosan consistently boosted callose levels, overall callose production varied according to the growth conditions. This environmental variability affected both basal callose deposition in mock-treated plants and PAMP-induced callose in Flg22- and chitosan-treated plants. Hence, the environmental growth conditions do not exclusively act on the responsiveness to PAMPs but, rather, affect the plant's overall capacity to deposit callose (Figs. 2 and 3). Remarkably, pretreatment with the environmental response hormone ABA had opposite effects on callose production, depending on the environmental growth conditions (Fig. 4). These results not only provide an explanation for the controversial role of ABA in callose defense (Ton et al. 2009), but they also complicate the interpretation of callose deposition as a uniform defense marker of PTI signaling. In support of that conclusion, we furthermore found that the pathways controlling Flg22- and chitosan-induced callose differ in their requirement for various signal transduction components. Hence, the model system of PAMP-induced callose in hydroponically grown *Arabidopsis* involves regulation by more than one pathway, which differs according to the environmental conditions and the eliciting PAMP. This outcome warrants extra caution with generalizations regarding PTI signaling on the basis of this model system.

Antioxidant vitamins suppressed callose deposition, whereas light intensity stimulated callose deposition (Fig. 2). The accumulation of H_2O_2 displayed remarkably similar pat-

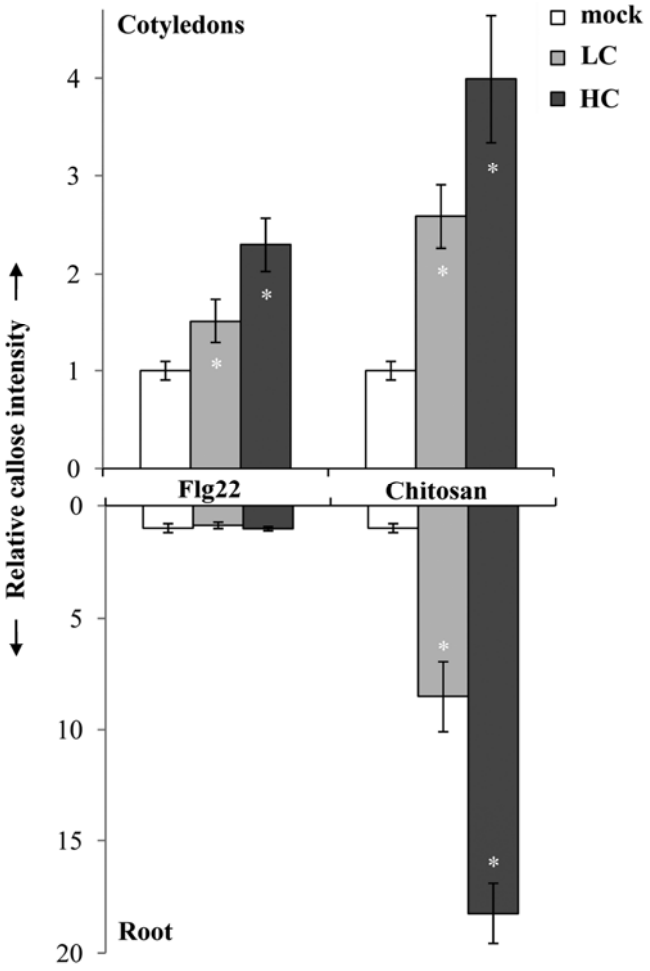

Fig. 7. Callose deposition in cotyledons and roots in response to Flg22 or chitosan. Data shown are average values (± standard error of the mean; $n > 20$) of relative callose intensities at 24 h after pathogen-associated molecular pattern (PAMP) treatment. Values were standardized to intensities in mock-treated tissues. Seedlings were treated with 5 µM abscissic acid at 24 h prior to PAMP treatment. Asterisks indicate statistically significant changes in response to PAMP treatment (Student's *t*-test; $\alpha = 0.05$). LC = low PAMP concentration, i.e., 0.2 µM Flg22 or 0.002% chitosan; HC = high PAMP concentration, i.e., 1 µM Flg22 or 0.01% chitosan.

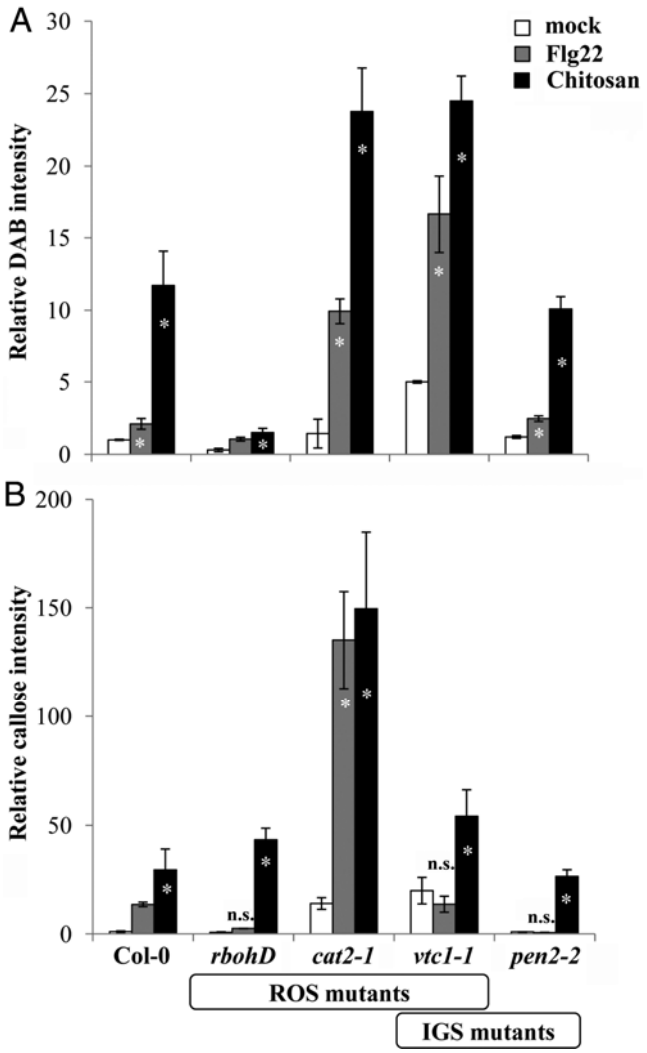

Fig. 8. Effect of mutations in homeostasis of reactive oxygen species (ROS) and biosynthesis of indolytic glucosinolates (IGS) on **A,** H_2O_2 production and **B,** callose deposition upon treatment with 1 µM Flg22 or 0.01% chitosan. Data shown are average values (± standard error of the mean; $n > 15$) of relative staining intensities. Values were standardized to staining intensities in mock-treated wild-type seedlings (Col-0). Seedlings were treated with 5 µM abscissic acid at 24 h prior to pathogen-associated molecular pattern (PAMP) treatment. Asterisks indicate statistically significant changes in response to PAMP treatment within each genotype (Student's *t*-test; $\alpha = 0.05$). n.s. = no statistically significant difference between mock- and PAMP-treated seedlings.

terns of variation at these growth conditions (Fig. 3), suggesting that the environmental variability in callose deposition is caused by fluctuations in ROS. In this context, the callose-promoting effects by exogenously applied ABA (Fig. 4; Table 2) can be explained by ABA-induced ROS (Ghassemian et al. 2008; Xing et al. 2008). Conversely, the observed suppression by sucrose (Fig. 2) can be explained by repression of photosynthesis activity and related ROS (Paul and Driscoll 1997; Sheen 1990). Two recent studies identified five PTI signaling components on the basis of a mutant screen in Elf18-induced repression of anthocyanins at high sucrose, demonstrating that the negative cross-talk between sucrose and PTI signaling acts in two directions (Lu et al. 2009; Saijo et al. 2009). All five "*PRIORITY IN SWEET LIFE*" genes (*PSL*) isolated from this mutant screen encode components in endoplasmatic reticulum-localized N-glycosylation, which regulates quality control and stable expression of the Elf18 receptor EFR. Interestingly however, the *psl* mutants were unaffected in stability and functioning of the Flg22 receptor FLS2 (Lu et al. 2009; Saijo et al. 2009), demonstrating that the involvement of N-glycosylation in PTI signaling is PAMP-specific (Haweker et al. 2010; Saijo 2010). In this study, we demonstrated a PAMP-specific contribution of signaling components further downstream in PTI signaling, such as AtRBOHD, glucosinolate metabolites, and even the callose synthase PMR4 (Figs. 8 and 9). Considering that single pathogen species produce multiple PAMP signals, we conclude that callose deposition in response to pathogen infection is regulated by multiple signaling pathways rather than one conserved downstream pathway.

The contrasting effects of ABA on callose regulation under different growth conditions point to a complex interplay between environmental signaling pathways. In our experiments, ABA repressed basal and PAMP-induced callose at low light intensity, high sucrose concentration and vitamins (Fig. 4), whereas all other conditions supported predominantly stimulatory effects by ABA (Fig. 4; Table 2). Previously, it was shown that ABA represses Flg22-induced callose in hydroponic *Arabidopsis* under nearly identical growth conditions (Clay et al. 2009), except for the concentration of sucrose in the growth medium (0.5%) (Clay et al. 2009). This callose suppression by ABA was explained by a repressed activity of the ethylene-inducible transcription factor MYB51, which regulates the biosynthesis of indolic glucosinolates (Gigolashvili et al. 2007). However, such cross-talk mechanism does not explain why ABA stimulates callose under other growth conditions. Interestingly, our study demonstrated that growth conditions supporting ABA-induced potentiation of callose allow for enhanced levels of H_2O_2 accumulation in the tissue (Figs. 3 and 4). Furthermore, exogenous application of ABA has been demonstrated to trigger H_2O_2 accumulation in *Arabidopsis* (Xing et al. 2008). We, therefore, propose that environmental growth conditions can boost ABA-induced ROS to a threshold that promotes callose, thereby masking or bypassing ABA-induced suppression of MYB51-dependent callose.

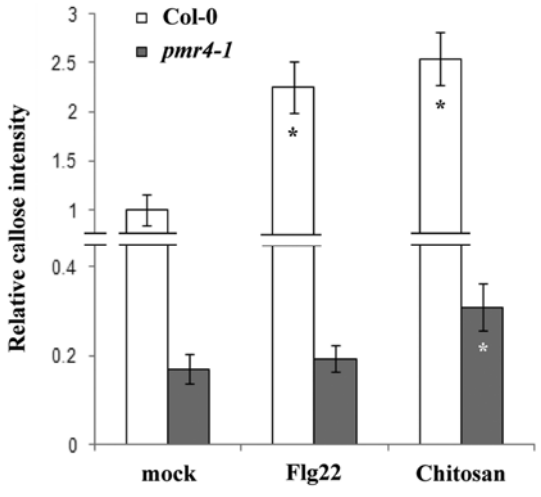

Fig. 9. Callose deposition in wild-type (Col-0) and *pmr4-1* seedlings at 24 h after treatment with 1 μM Flg22, or 0.01 % chitosan. Asterisks indicate statistically significant changes in response to pathogen-associated molecular pattern (PAMP) treatment within each genotype (Student's *t*-test: $\alpha = 0.05$). n.s. = no statistically significant difference between mock- and PAMP-treated seedlings.

The analysis of *Arabidopsis* signaling mutants revealed that the *cat2-1* mutant accumulates significantly enhanced levels of H_2O_2 and callose after treatment with Flg22 or chitosan (Fig. 8). Considering that *cat2-1* is impaired in a peroxisomal catalase (Bueso et al. 2007), this mutant phenotype confirms a potentiating role of H_2O_2 in both Flg22- and chitosan-induced callose. We furthermore found that the *rbohD* mutant is blocked in Flg22-induced callose but not in chitosan-induced callose (Fig. 8B), whereas both Flg22- and chitosan-induced H_2O_2 were dramatically reduced in this mutant (Fig. 8A). Hence, chitosan-induced callose does not require H_2O_2 from the NADPH oxidase RBOHD. Furthermore, *rbohD* seedlings still showed a statistically significant increase in H_2O_2 after PAMP treatment, despite the obvious reduction in absolute H_2O_2 levels compared with wild-type plants. This demonstrates that PAMP-induced H_2O_2 is only partially derived from RBOHD. Consequently, we propose that Flg22-induced callose, like OG-induced callose (Galletti et al. 2008), is controlled by RBOHD-dependent H_2O_2, whereas chitosan-induced callose is controlled by RBOHD-independent H_2O_2. Additional evidence for differential regulation of Flg22- and chitosan-induced callose comes from the behavior of the *pen2-2* and *vtc1-1* mutants. Both mutants were blocked in Flg22-induced callose but were unaffected in chitosan-induced callose (Fig. 8B). Given the role of PEN2 and VTC1 in the hydrolysis of glucosinolates (Bednarek et al. 2009; Burmeister et al. 2000; Clay et al. 2009), we support the conclusion that Flg22-induced callose is regulated by glucosinolate-derived metabolites. However, these metabolites are apparently not involved in the regulation of chitosan-induced callose.

Chitosan has long been known for its defense-eliciting capacities in plants, even though the nature and intensity of the chitosan-induced plant defense response differs according to its physiochemical characteristics, such as degree of de-acytelation, viscosity, and molecular weight (Iritri and Faoro 2009). In this study, we have used low-viscous chitosan with a molecular weight of approximately 150 kDa and a 95 to 98% degree of acetylation (Hombach and Bernkop-Schnürch 2009). The only mutation that significantly reduced chitosan-induced callose was the *pmr4-1* mutation (Fig. 9). Conversely, mutations affecting the plant's ROS-scavenging ability, such as *cat2-1* and *vtc1-1*, allowed for augmented levels of chitosan-induced callose (Fig. 8). Furthermore, both Flg22- and chitosan-induced callose were consistently higher under environmental growth conditions that allowed for higher levels of ROS accumulation (Figs. 2 and 3). Hence, despite the specific differences between the pathways controlling Flg22- and chitosan-induced callose, ROS seem to have a potentiating effect on callose production in general.

The Flg22 response of *Arabidopsis* has emerged as a widely used model system to study PTI signaling. Recognition of Flg22 triggers a rapid mitogen-activated protein kinase (MAPK) cascade involving the defense regulatory kinases MAPK3 and MAPK6 (Asai et al. 2002; Suarez-Rodriguez et al. 2007), which can be suppressed by virulence-promoting

pathogen effectors (He et al. 2006; Zhang et al. 2007). This MPK3- and MPK6-dependent MAPK cascade activates downstream WRKY transcription factors that promote transcription of early-acting defense genes (Asai et al. 2002; Navarro et al. 2004). In addition, this MAPK cascade stimulates generation of RBOHD-dependent ROS, which subsequently promote deposition of PMR4-dependent callose (He et al. 2006; Zhang et al. 2007). The recent discovery that glucosinolate metabolites regulate Flg22-induced callose adds a novel layer to signaling pathways controlling this PTI response (Clay et al. 2009). Given the toxic nature of glucosinolate break-down products (Halkier and Gershenzon 2006), their function in callose deposition may be explained as part of a cellular detoxification response, which mediates secretion of these defense metabolites into the apoplast, in which they are captured in callose-containing papillae. Accordingly, glucosinolate metabolites act at relatively late stages of the Flg22-induced pathway. In support of this, we found that *vtc1-1* and *pen2-2* are not reduced in Flg22-induced H_2O_2, suggesting that glucosinolate metabolites act downstream of RBOHD-generated H_2O_2 in the regulation of Flg22-induced callose.

Unlike other studies, our experiments revealed relatively high basal levels of callose in the mock treatments. Apart from differences in growth conditions, this discrepancy could be related to a difference in staining technique. Whereas our experiments used ethanol for the destaining of green tissues, other studies commonly use ethanol followed by treatment with 10% NaOH for this purpose (Clay et al. 2009; Millet et al. 2010). It is possible that incubation in such a strongly alkaline solution removes or eradicates part of the callose that is present at the cell wall, thereby lowering the detection limit of callose and giving the impression that cotyledons from mock-treated plants contain no callose. Another surprising outcome was the lack of Flg22-induced callose in roots, which contradicts a recent report by Millet and associates (2010), who demonstrated that Flg22-induced callose in *Arabidopsis* roots depends on a similar pathway as Flg22-induced callose in cotyledons (Clay et al. 2009). It seems difficult to envisage that our staining method fails to detect Flg22-induced callose in the roots while is suitable for detection of basal and chitosan-induced callose in the roots. It is, therefore, more plausible that this discrepancy originates from differences in growth conditions. Whereas Millet and associates (2010) cultivated seedlings in Murashige Skoog (MS) medium with vitamins at a light intensity of 100 $\mu E\ m^{-2}\ s^{-1}$, we cultivated the seedlings in medium without vitamins at 150 $\mu E\ m^{-2}\ s^{-1}$ of light. Since higher levels of light and lack of vitamins allow for significantly higher levels of basal ROS and callose accumulation (Figs. 2B and 3), we propose that Flg22-induced callose in roots was masked by relatively high basal levels of callose deposition under our experimental conditions.

In summary, our study uncovered an unexpectedly large degree of environmental variation in callose deposition of hydroponically grown *Arabidopsis*. It is of concern that this model system is widely used to study PTI signaling and seems to be designed to minimise experimental variation. It can, therefore, be expected that fluctuations in environmental growth conditions have even bigger impacts on PTI signaling during more complex interactions, such as those between soil-grown plants and pathogenic microbes or plant-beneficial microbes or both. This could also explain the previously reported controversy about the involvement of plant hormones in plant-microbe interactions (Beckers and Spoel 2006; Robert-Seilaniantz et al. 2007; Ton et al. 2009) as well as inconsistencies in complex plant-microbe assays. Above all, our study warrants the use of extra caution with generalizations regarding plant innate immunity on the basis of callose deposition in hydroponically grown *Arabidopsis* seedlings.

MATERIALS AND METHODS

Plant material, growth conditions, and chemical treatments.

Seeds of *Arabidopsis thaliana* accession Col-0 and mutants in this background (*pmr4-1* [Nishimura et al. 2003], *vtc1-1* [Conklin et al. 2000], *cat2-1* [Bueso et al. 2007], *pen2-2* [Lipka et al. 2005], and *rbohD* [Pogany et al. 2009]) were vapor-phase sterilized for 4 to 6 h (S. Clough and A. Bent, *personal communication*). Approximately 15 seeds per well were planted in sterile 12-well plates, each containing 1 ml of filter-sterilized basal MS medium with or without Gamborg vitamins (Sigma) (containing 100 μg of myo-inositol per liter, 1 μg of nicotinic acid per liter, 1 μg of pyridoxine hydrochloride per liter, and 10 μg of thiamine hydrochloride per liter) with varying concentrations of sucrose (0, 1, 2.5, and 5%). All growth media were supplemented with 0.5% morpholineethanesulfonic acid hydrate (final pH = 5.7 to 5.8). Plates were kept in the dark at 4°C for 1 to 2 days before being transferred to controlled growth cabinets. Seedlings were cultivated under standard growth conditions (16-h-day and 8-h-night cycle; 20°C and 17°C, respectively) at two different light intensities (75 and 150 $\mu E\ m^{-2}\ s^{-1}$). At 7 days of growth, MS medium was replaced with fresh medium. ABA was applied at day 8 to a final concentration to 5 or 50 μM. At day 9, seedlings were challenged with 1 μM Flg22 (applied as 10 μl of 100 μM Flg22 solution) (GenScript, Piscataway, NJ, U.S.A.) or 0.01% (wt/vol) low-viscous chitosan (Fluka, Milwaukee, WI, U.S.A.) (applied as 10 μl of 1% chitosan (vol/wt) solution in 1% acetic acid), which has a molecular weight of approximately 150 kDa and a 95 to 99.8% degree of acetylation (Hombach and Bernkop-Schnürch 2009). These PAMP concentrations were based on previously reported dose-response experiments (Flg22, Gomez-Gomez et al. 1999b; chitosan, Iriti et al. 2006), as well as the consistency in callose responses between independent experiments (data not shown). Mock treatments were performed by the addition of 10 μl of water to the growth medium. Addition of 10 μl of 1% acetic acid did not change the pH nor influence callose deposition in mock- or Flg22-treated plants (data not shown). Experiments to examine callose deposition under different growth and ABA conditions were performed at three different laboratories, at Rothamsted Research, Harpenden, U.K., at the University of Jaume I of Castellón, Spain, and at the University of Neuchâtel, Switzerland.

Aniline blue staining, microscopy analysis, and callose quantification.

Seedlings were collected, destained in 95% EtOH and stained with aniline-blue as described previously, with some modification (Ton et al. 2005). Briefly, seedlings were incubated for at least 24 h in 95 to 100% ethanol until all tissues were transparent, were washed in 0.07 M phosphate buffer (pH =9), and were incubated for 1 to 2 h in 0.07 M phosphate buffer containing 0.01% aniline-blue (Sigma, St. Louis), prior to microscopic analysis. Observations were performed with an epifluorescence microscope with UV filter (BP 340 to 380 nm, LP 425 nm). Callose was quantified from digital photographs by the number of white pixels (callose intensity) or the number of depositions relative to the total number of pixels covering plant material, using Photoshop CS2 software. Contrast settings of the photographs were adjusted to obtain an optimal separation of the callose signal from the background signal (Supplementary Fig. S3). Callose was selected automatically, using the "Color Range" tool. In cases in which the contrast settings resulted in significant loss of callose signal due to high autofluorescence signals from the vasculature, callose was selected manually, using the "Magic Wand" tool of Photoshop CS3. The accuracy of the resulting callose selection was visu-

ally verified before proceeding. Callose-corresponding pixels and numbers of depositions were recorded as the area covered by the total number of selected pixels and the number of measurements, respectively, using the "Record Measurements" tool of Photoshop CS3. Average callose measurements were based on at least 20 photographs from different seedlings and were analyzed for statistical differences by Student's *t*-tests or analysis of variance following by Fisher's least significant differences tests ($n = 20$ to 40; $\alpha = 0.05$).

DAB staining, microscopy analysis, and H_2O_2 quantification. Seedlings were stained in 1 mg of DAB per milliliter at pH < 3 for 24 h in the dark and were subsequently destained in chloral-hydrate, as described previously (Thordal-Christensen et al. 1997). DAB staining intensities were quantified from digital photographs (Nikon Eclipse 11000, Tokyo) by the number of dark-brown DAB pixels relative to total pixels corresponding to plant material, using Photoshop CS3. Analysis for statistical differences were performed as described for the callose quantifications. For double staining of H_2O_2 and callose, plant material was stained with DAB as described above but was destained in 95% ethanol instead of chloral-hydrate. Subsequently, samples were stained with aniline-blue, as described above.

ACKNOWLEDGMENTS

We thank F. Mauch for helpful comments and suggestions to earlier versions of this manuscript. This research was supported by a Leonardo Da Vinci grant to E. Luna and a BBSRC Institute Career Path Fellowship (number BB/E023959/1) to J. Ton. We thank the Swiss National Foundation for supporting B. Mauch-Mani (grant 31003A-120197) and the Plan de Promoción Bancaja-UJI P1.1A2007-07 and the Generalitat Valenciana GV/2007/099 for funding V. Flors. We are grateful to P. García for her support (AGL-2007-66282-C02-02).

LITERATURE CITED

Adams-Phillips, L., Briggs, A. G., and Bent, A. F. 2010. Disruption of poly(ADP-ribosyl)ation mechanisms alters responses of Arabidopsis to biotic stress. Plant Physiol. 152:267-280.

Asai, T., Tena, G., Plotnikova, J., Willmann, M. R., Chiu, W. L., Gomez-Gomez, L., Boller, T., Ausubel, F. M., and Sheen, J. 2002. MAP kinase signalling cascade in Arabidopsis innate immunity. Nature 415:977-983.

Asselbergh, B., De Vleesschauwer, D., and Hofte, M. 2008. Global switches and fine-tuning-ABA modulates plant pathogen defense. Mol. Plant-Microbe Interact. 21:709-719.

Beckers, G. J., and Spoel, S. H. 2006. Fine-tuning plant defence signalling: salicylate versus jasmonate. Plant Biol. (Stuttg) 8:1-10.

Bednarek, P., Pislewska-Bednarek, M., Svatos, A., Schneider, B., Doubsky, J., Mansurova, M., Humphry, M., Consonni, C., Panstruga, R., Sanchez-Vallet, A., Molina, A., and Schulze-Lefert, P. 2009. A glucosinolate metabolism pathway in living plant cells mediates broad-spectrum antifungal defense. Science 323:101-106.

Boller, T., and Felix, G. 2009. A renaissance of elicitors: Perception of microbe-associated molecular patterns and danger signals by pattern-recognition receptors. Annu. Rev. Plant Biol. 60:379-406.

Brown, I., Trethowan, J., Kerry, M., Mansfield, J., and Bolwell, G. P. 1998. Localization of components of the oxidative cross-linking of glycoproteins and of callose synthesis in papillae formed during the interaction between non-pathogenic strains of *Xanthomonas campestris* and French bean mesophyll cells. Plant J. 15:333-343.

Bueso, E., Alejandro, S., Carbonell, P., Perez-Amador, M. A., Fayos, J., Bellés, J. M., Rodriguez, P. L., and Serrano, R. 2007. The lithium tolerance of the Arabidopsis *cat2* mutant reveals a cross-talk between oxidative stress and ethylene. Plant J. 52:1052-1065.

Burmeister, W. P., Cottaz, S., Rollin, P., Vasella, A., and Henrissat, B. 2000. High resolution X-ray crystallography shows that ascorbate is a cofactor for myrosinase and substitutes for the function of the catalytic base. J. Biol. Chem. 275:39385-39393.

Clay, N. K., Adio, A. M., Denoux, C., Jander, G., and Ausubel, F. M. 2009. Glucosinolate metabolites required for an Arabidopsis innate immune response. Science 323:95-101.

Conklin, P. L., Saracco, S. A., Norris, S. R., and Last, R. L. 2000. Identification of ascorbic acid-deficient *Arabidopsis thaliana* mutants. Genetics 154:847-856.

de Torres-Zabala, M., Truman, W., Bennett, M. H., Lafforgue, G., Mansfield, J. W., Rodriguez Egea, P., Bogre, L., and Grant, M. 2007. Pseudomonas syringae pv. tomato hijacks the Arabidopsis abscisic acid signalling pathway to cause disease. EMBO (Eur. Mol. Biol. Organ.) J. 26:1434-1443.

Dunning, F. M., Sun, W., Jansen, K. L., Helft, L., and Bent, A. F. 2007. Identification and mutational analysis of Arabidopsis FLS2 leucine-rich repeat domain residues that contribute to flagellin perception. Plant Cell 19:3297-3313.

Flors, V., Ton, J., Jakab, G., and Mauch-Mani, B. 2005. Abscisic acid and callose: Team players in defence against pathogens? J. Phytopathol. 153:377-383.

Fu, Z. Q., Guo, M., Jeong, B. R., Tian, F., Elthon, T. E., Cerny, R. L., Staiger, D., and Alfano, J. R. 2007. A type III effector ADP-ribosylates RNA-binding proteins and quells plant immunity. Nature 447:284-288.

Galletti, R., Denoux, C., Gambetta, S., Dewdney, J., Ausubel, F. M., De Lorenzo, G., and Ferrari, S. 2008. The AtrbohD-mediated oxidative burst elicited by oligogalacturonides in Arabidopsis is dispensable for the activation of defense responses effective against *Botrytis cinerea*. Plant Physiol. 148:1695-1706.

Gamborg, O. L., Miller, R. A., and Ojima, K. 1968. Nutrient requirements of suspension cultures of soybean root cells. Exp. Cell Res. 50:151-158.

Ghassemian, M., Lutes, J., Chang, H. S., Lange, I., Chen, W., Zhu, T., Wang, X., and Lange, B. M. 2008. Abscisic acid-induced modulation of metabolic and redox control pathways in *Arabidopsis thaliana*. Phytochemistry 69:2899-2911.

Gigolashvili, T., Berger, B., Mock, H. P., Muller, C., Weisshaar, B., and Flugge, U. I. 2007. The transcription factor HIG1/MYB51 regulates indolic glucosinolate biosynthesis in Arabidopsis thaliana. Plant J. 50:886-901.

Gomez-Gomez, L., and Boller, T. 2000. FLS2: An LRR receptor-like kinase involved in the perception of the bacterial elicitor flagellin in Arabidopsis. Mol. Cell 5:1003-1012.

Gomez-Gomez, L., Felix, G., and Boller, T. 1999a. A single locus determines sensitivity to bacterial flagellin in *Arabidopsis thaliana*. Plant J. 18:277-284.

Gomez-Gomez, L., Felix, G., and Boller, T. 1999b. A single locus determines sensitivity to bacterial flagellin in *Arabidopsis thaliana*. Plant J. 18:277-284.

Halkier, B. A., and Gershenzon, J. 2006. Biology and biochemistry of glucosinolates. Annu. Rev. Plant Biol. 57:303-333.

Haweker, H., Rips, S., Koiwa, H., Salomon, S., Saijo, Y., Chinchilla, D., Robatzek, S., and von Schaewen, A. 2010. Pattern recognition receptors require N-glycosylation to mediate plant immunity. J. Biol. Chem. 285:4629-4636.

He, P., Shan, L., Lin, N.-C., Martin, G. B., Kemmerling, B., Nürnberger, T., and Sheen, J. 2006. Specific bacterial suppressors of MAMP signaling upstream of MAPKKK in Arabidopsis innate immunity. Cell 125:563-575.

Hombach, J., and Bernkop-Schnürch, A. 2009. Chitosan solutions and particles: Evaluation of their permeation enhancing potential on MDCK cells used as blood brain barrier model. Int. J. Pharm. 376:104-109.

Iriti, M., Sironi, M., Gomarasca, S., Casazza, A. P., Soave, C., and Faoro, F. 2006. Cell death-mediated antiviral effect of chitosan in tobacco. Plant Physiol. Biochem. 44:893-900.

Iritri, M., and Faoro, F. 2009. Chitosan as a MAMP, searching for a PRR. Plant , Signal. Behav. 4:66-68.

Jeworutzki, E., Roelfsema, M. R., Anschutz, U., Krol, E., Elzenga, J. T., Felix, G., Boller, T., Hedrich, R., and Becker, D. 2010. Early signaling through the Arabidopsis pattern recognition receptors FLS2 and EFR involves Ca(2+)-associated opening of plasma membrane anion channels. Plant J. 62: 367-378.

Kohler, A., Schwindling, S., and Conrath, U. 2002. Benzothiadiazole-induced priming for potentiated responses to pathogen infection, wounding, and infiltration of water into leaves requires the NPR1/NIM1 gene in Arabidopsis. Plant Physiol. 128:1046-1056.

Kunze, G., Zipfel, C., Robatzek, S., Niehaus, K., Boller, T., and Felix, G. 2004. The N terminus of bacterial elongation factor Tu elicits innate immunity in Arabidopsis plants. Plant Cell 16:3496-3507.

Li, Y., Zhang, Q., Zhang, J., Wu, L., Qi, Y., and Zhou, J.-M. 2010. Identification of microRNAs involved in pathogen-associated molecular pattern-triggered plant innate immunity. Plant Physiol. 152:2222-2231.

Lipka, V., Dittgen, J., Bednarek, P., Bhat, R., Wiermer, M., Stein, M., Landtag, J., Brandt, W., Rosahl, S., Scheel, D., Llorente, F., Molina, A., Parker, J., Somerville, S., and Schulze-Lefert, P. 2005. Pre- and postinvasion defenses both contribute to nonhost resistance in Arabidopsis. Science 310:1180-1183.

Lu, X., Tintor, N., Mentzel, T., Kombrink, E., Boller, T., Robatzek, S.,

Schulze-Lefert, P., and Saijo, Y. 2009. Uncoupling of sustained MAMP receptor signaling from early outputs in an Arabidopsis endoplasmic reticulum glucosidase II allele. Proc. Natl. Acad. Sci. U.S.A. 106:22522-22527.

Mauch-Mani, B., and Mauch, F. 2005. The role of abscisic acid in plant-pathogen interactions. Curr. Opin. Plant Biol. 8:409-414.

Millet, Y. A., Danna, C. H., Clay, N. K., Songnuan, W., Simon, M. D., Werck-Reichhart, D., and Ausubel, F. M. 2010. Innate immune responses activated in Arabidopsis roots by microbe-associated molecular patterns. Plant Cell 22:973-990.

Navarro, L., Zipfel, C., Rowland, O., Keller, I., Robatzek, S., Boller, T., and Jones, J. D. 2004. The transcriptional innate immune response to flg22. Interplay and overlap with Avr gene-dependent defense responses and bacterial pathogenesis. Plant Physiol. 135:1113-1128.

Nicaise, V., Roux, M., and Zipfel, C. 2009. Recent advances in PAMP-triggered immunity against bacteria: Pattern recognition receptors watch over and raise the alarm. Plant Physiol. 150:1638-1647.

Nishimura, M. T., Stein, M., Hou, B. H., Vogel, J. P., Edwards, H., and Somerville, S. C. 2003. Loss of a callose synthase results in salicylic acid-dependent disease resistance. Science 301:969-972.

Paul, M. J., and Driscoll, S. P. 1997. Sugar repression of photosynthesis: The role of carbohydrates in signalling nitrogen deficiency through source:sink imbalance. Plant Cell Environ. 20:110-116.

Pogany, M., von Rad, U., Grun, S., Dongo, A., Pintye, A., Simoneau, P., Bahnweg, G., Kiss, L., Barna, B., and Durner, J. 2009. Dual roles of reactive oxygen species and NADPH oxidase RBOHD in an Arabidopsis-Alternaria pathosystem. Plant Physiol. 151:1459-1475.

Ridley, B. L., O'Neill, M. A., and Mohnen, D. 2001. Pectins: Structure, biosynthesis, and oligogalacturonide-related signaling. Phytochemistry 57:929-967.

Robatzek, S., Chinchilla, D., and Boller, T. 2006. Ligand-induced endocytosis of the pattern recognition receptor FLS2 in Arabidopsis. Genes Dev. 20:537-542.

Robert-Seilaniantz, A., Navarro, L., Bari, R., and Jones, J. D. 2007. Pathological hormone imbalances. Curr Opin Plant Biol 10:372-9.

Saijo, Y. 2010. ER quality control of immune receptors and regulators in plants. Cell Microbiol. 12: 716-724.

Saijo, Y., Tintor, N., Lu, X., Rauf, P., Pajerowska-Mukhtar, K., Haweker, H., Dong, X., Robatzek, S., and Schulze-Lefert, P. 2009. Receptor quality control in the endoplasmic reticulum for plant innate immunity. EMBO (Eur. Mol. Biol. Organ.) J. 28:3439-3449.

Sheen, J. 1990. Metabolic repression of transcription in higher plants. Plant Cell 2:1027-1038.

Suarez-Rodriguez, M. C., Adams-Phillips, L., Liu, Y., Wang, H., Su, S.-H., Jester, P. J., Zhang, S., Bent, A. F., and Krysan, P. J. 2007. MEKK1 Is Required for flg22-induced MPK4 activation in Arabidopsis plants. Plant Physiol. 143:661-669.

Thordal-Christensen, H., Zhang, Z., Wei, Y., and Collinge, D. B. 1997. Subcellular localization of H_2O_2 in plants. H_2O_2 accumulation in papillae and hypersensitive response during the barley-powdery mildew interaction. Plant J. 11:1187-1194.

Ton, J., Flors, V., and Mauch-Mani, B. 2009. The multifaceted role of ABA in disease resistance. Trends Plant Sci. 14:310-317.

Ton, J., Jakab, G., Toquin, V., Flors, V., Iavicoli, A., Maeder, M. N., Metraux, J. P., and Mauch-Mani, B. 2005. Dissecting the beta-aminobutyric acid-induced priming phenomenon in Arabidopsis. Plant Cell 17:987-999.

Ton, J., and Mauch-Mani, B. 2004. Beta-amino-butyric acid-induced resistance against necrotrophic pathogens is based on ABA-dependent priming for callose. Plant J. 38:119-130.

Wang, L., Tsuda, K., Sato, M., Cohen, J. D., Katagiri, F., and Glazebrook, J. 2009. Arabidopsis CaM binding protein CBP60g contributes to MAMP-induced SA accumulation and is involved in disease resistance against *Pseudomonas syringae*. PLoS Pathog 5:e1000301. Published online.

Xing, Y., Jia, W., and Zhang, J. 2008. AtMKK1 mediates ABA-induced *CAT1* expression and H_2O_2 production via AtMPK6-coupled signaling in Arabidopsis. Plant J. 54:440-451.

Yakushiji, S., Ishiga, Y., Inagaki, Y., Toyoda, K., Shiraishi, T., and Ichinose, Y. 2009. Bacterial DNA activates immunity in Arabidopsis thaliana. J. Gen. Plant Pathol. 75:227-234.

You, M. K., Shin, H. Y., Kim, Y. J., Ok, S. H., Cho, S. K., Jeung, J. U., Yoo, S. D., Kim, J. K., and Shin, J. S. 2010. Novel bifunctional nucleases, OmBBD and AtBBD1, are involved in abscisic acid-mediated callose deposition in Arabidopsis. Plant Physiol. 152:1015-1029.

Zhang, J., Shao, F., Li, Y., Cui, H., Chen, L., Li, H., Zou, Y., Long, C., Lan, L., Chai, J., Chen, S., Tang, X., and Zhou, J. M. 2007. A Pseudomonas syringae effector inactivates MAPKs to suppress PAMP-induced immunity in plants. Cell Host Microbe 1:175-185.

Zimmerli, L., Jakab, G., Métraux, J.-P., and Mauch-Mani, B. 2000. Potentiation of pathogen-specific defense mechanisms in Arabidopsis by β-aminobutyric acid. Proc. Natl. Acad. Sci. U.S.A. 97:12920-12925.